The 2010 IEEE/RSJ International Conference on
Intelligent Robots and Systems
October 18-22, 2010, Taipei, Taiwan

A Novel Stair-Climbing Wheelchair with Transformable Wheeled Four-Bar Linkages

Yusuke Sugahara, Naoaki Yonezawa and Kazuhiro Kosuge

Abstract— **This paper describes the development of a novel multi-wheel stair-climbing wheelchair. The necessity for mobility aid technology for elderly and handicapped people that has "minimal invasiveness for use in an historical environment" is described. With this goal in mind, a prototype of a novel wheelchair having a stair-climbing function resulting from transformable wheeled four-bar linkages is proposed. The mechanical design, principle of operation and statics of the proposed mechanism are thoroughly illustrated. The basic performance of the proposed mechanism has been confirmed through experimental results.**

I. Introduction

Recently, in order to create a society in which it is easy for elderly and disabled people to be self-reliant and participate, the "barrier-free" concept has been disseminated, and the scope of activity of elderly and disabled wheelchair users has been expanded. However, when considering environments having important cultural meanings, such as historical buildings as well as cultural heritage and historical sites, from the viewpoint of authenticity [12], [1] and historical value, it is not desirable to remove existing barriers by improving the infrastructure by means such as installing elevators. Especially in Japan, where most historical buildings are of wooden construction, it is very difficult to make such facilities barrier free without damaging the heritage itself, thus multistoried historical buildings designated as national treasures remain, as of today, inaccessible to wheelchair users. As for a barrier-free methodology for historical environments that does not damage the authenticity of a structure or site, although there have recently been a few studies that point out problems in terms of architectonics [19], [16], there have been no reports on technical research and development into this problem.

The final target of our research involves realizing a smooth and hospitable means of locomotion for wheelchair users in environments having a cultural meaning, such as historical Japanese wooden buildings and castle ruins, without tampering with the authenticity of the environment. Our research is, in a manner, the development of mobility aid technology having minimal invasiveness for use in an historical environment. In particular, the purpose of this research is to develop a wheelchair that contributes to independent locomotion for wheelchair users in an historical environment without tampering with the environment, and causing only the same amount of damage as a human walking in the environment, on historically authentic pathways, including stairs and uneven terrain.

There are many studies on stair-climbing wheelchairs as a methodology for a barrier-free society. First there is Patra Four [6], which can climb steps having risers of more than 80 mm, and which is a fine example of an electric wheelchair having the capacity to function on uneven ground, although it cannot go up stairs. Next is the HELIOS-V [15], which has ability to climb stairs using special wheels, however, this wheelchair applies a concentrated load on the front edge of stair treads, which damages wooden buildings. A stair-climbing wheelchair using a rotary cross arm with wheels [18] is sophisticated, but it is difficult to operate in narrow historical buildings because the wheelchair has a long wheelbase, and cannot turn when climbing. The famous electric wheelchair "iBOT" [8] is capable of ascending and descending stairs as well as slopes, but it applies a high ground pressure and is difficult to be utilized in wooden buildings because only two wheels are landed when ascending and descending stairs. The iBOT also has another demerit in that stability during climbing is not ensured. The Stair-Climbing Wheelchair [9] and Zero Carrier [20], [2], which have similar mechanism, are also sophisticated stair-climbing vehicles that adapt to various step heights and treads with a

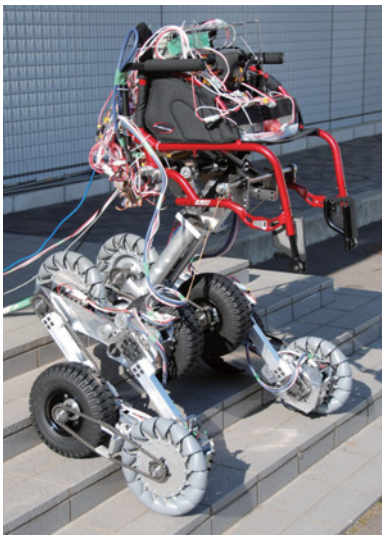

Fig. 1. TBW-1 Matsushima.

This research was done as an collaboration research in Aoba Foundation for The Promotion of Engineering, and partially supported by MEXT Grant-in-Aid for Young Scientists (B) 20760157. The basic idea has been based on discussion with K. Yamada, T. Kano, M. Muranaka, Y. Azechi, M. Aikawa, K. Hashimoto, T. Sawato, A. Hayashi, N. Endo, S. Momoki, K. Hattori, A. Shimomura, N. Sakakibara, J. Shimizu, Y. Tokunaga, K. Aida and A. Takanishi. The authors would like to thank them.

Y. Sugahara, N. Yonezawa and K. Kosuge are with Department of Bioengineering and Robotics, Tohoku University, Sendai 980-8579, Japan. sugahara@irs.mech.tohoku.ac.jp

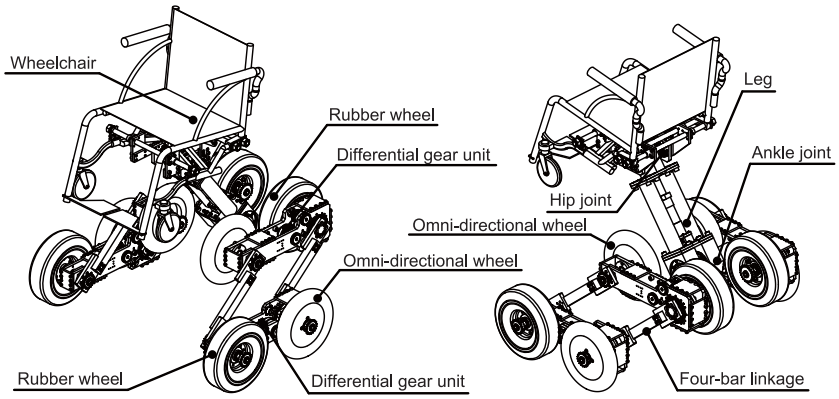

Fig. 2. Outline of TBW-1 Matsushima.

wide support polygon. However, they have too many DOF and have difficulty in traveling over uneven terrain because it is essentially impossible for them to use large wheels. CALMOS [3], which has a four-bar based mechanism to climb steps and stairs, is one of simple and stable solutions, however, is also difficult to use large wheels. The HELIOS-VI [5], which is a stair-climbing vehicle having a simple structure that utilizes crawlers and passive wheels, also applies a concentrated load on the edges of the stair treads. Top Chair [13], which is a stair-climbing wheelchair using crawlers, is the same. Although the WL-16 [10], i-foot [14], HUBO FX-1 [7] and other biped vehicles are challenging the problem and can reduce damage to the environment to the same level as a walking human, they have several problems in terms of safety and locomotion efficiency.

In Japanese historical buildings and sites, it is desirable that a wheelchair does only the same amount of damage as a human walking in the environment. Therefore, it is necessary for a wheelchair to travel and to climb stairs at a low ground pressure–the same as a human walking–and not to apply a concentrated load on the front edge of the stair treads. Furthermore, it is necessary for the wheelchair to have the ability to turn while climbing in order to cope with stairs that twist, as well as the ability to traverse uneven terrain to travel historically authentic pathways. On the other hand, from the point of view of safety, it is necessary to ensure static stability at all times while climbing stairs.

With this goal in mind, the authors propose a novel stair-climbing wheelchair with wheeled transformable four-bar linkages as shown in Fig. 1. In this paper, the mechanism design, principle of operation and statics of the proposed mechanism are thoroughly illustrated, while kinematics has been already reported [11]. The basic performance of the proposed mechanism has been confirmed through experiments.

II. Design and Principle of Operation

Fig. 2 shows an outline of the developed wheelchair named as "TBW-1 Matsushima," which has a wheeled transformable stair-climbing mechanism. Its upper structure is derived from a commercially available wheelchair. The leg section has active upper pitch joint (hip joint) and lower pitch joint (ankle joint). The hip joint is connected under the seating face of upper body below the total COG of the upper structure and passenger, and the ankle joint connects to the right and left wheel four-bar linkage modules.

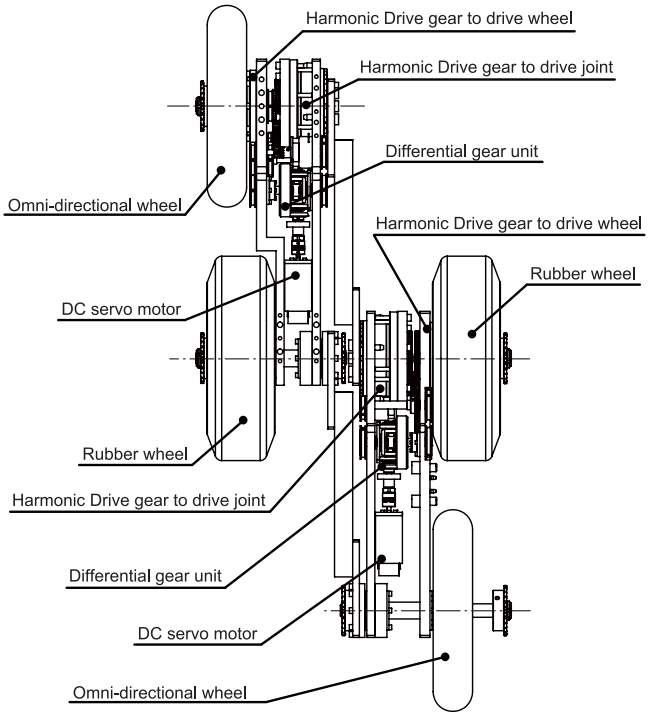

Fig. 3. Outline of Wheeled four-bar linkage module.

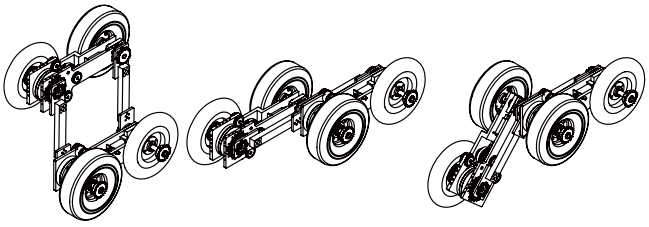

Fig. 4. Transformation of the wheeled four-bar linkage module. (a): Parallelogram mode, (b): Straight mode, (c): Dogleg mode.

The structure of the wheeled four-bar linkage module is shown in Fig. 3. This mechanism has four wheels at each vertex, and the adjacent two joints are active joints. By driving these active joints, this mechanism can transform

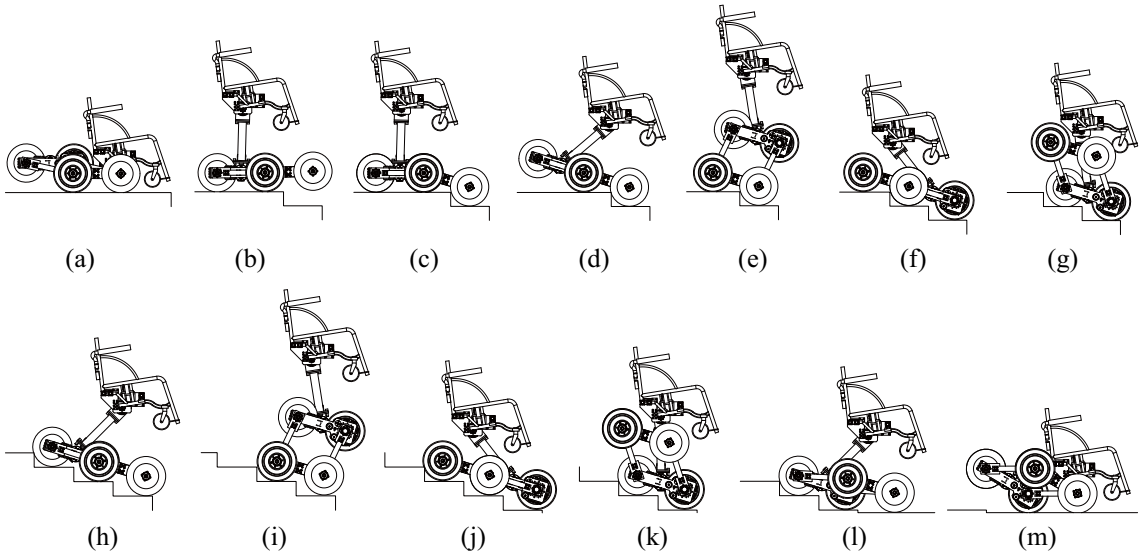

Fig. 5. Motion sequence of descending stairs.

itself from Parallelogram mode (Fig. 4(a)) to Straight mode (Fig. 4(b)). As the lengths of the four links are equal, it can also transform to Dogleg mode (Fig. 4(c)).

The motion sequence to ascend and descend stairs is shown in Fig. 5. The wheelchair basically goes stairs by repeating the transformation between Parallelogram mode and Straight mode. At least four wheels are in contact with the treads at all times when ascending and descending stairs, and this theoretically enables a lower ground-contact pressure and a wide support polygon than iBOT. Here, stability is ensured by controlling the joints to maintain a ZMP [17] located near the center of this support polygon. As shown in (c), Dogleg mode is utilized at the beginning of descending stairs and at the end of ascending stairs. In addition, half of the eight wheels are omni-directional wheels, and this enables the wheelchair to turn anytime as well as Patra Four, whether on stairs or on the road.

To drive this wheeled four-bar linkage mechanism, generally three actuators are needed: one for driving the wheels and two for driving the configuration. However in this study, a reduction in the number of actuators has been attempted by using Coupled Actuation [4] of joints and wheels with two actuators. Fig. 6 shows the structure of this mechanism. Motors are attached to the two parallel links, and the output of each motor is distributed by a differential gear unit to two motions: rotation of the wheels, and actuation of the adjacent two active joints. The angles of the joints are geometrically coupled, and the angles of the four wheels connected by a timing belt are equal. Here, the two output axes from one differential gear unit only are connected to the wheel axis and joint axis via a timing belt and spur gears, respectively. Therefore, the joints are actuated and the configuration of the four-bar linkage is varied when the two motors rotate in the same direction, and the joints are fixed and the wheels are driven when the motors rotate in opposite directions. The wheel axes and joint axes have Harmonic Drive gears, and this enables the choice of an appropriate reduction ratio for either stair-climbing or normal operation.

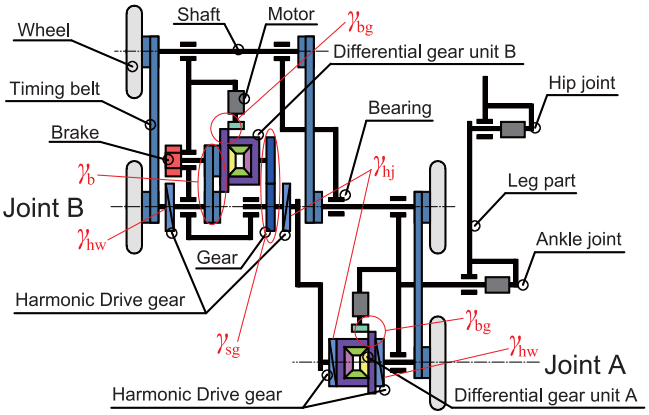

Fig. 6. Structure of wheeled four-bar linkage mechanism.

Because there are two postures in the Dogleg mode, the two adjacent active joints can drive the configuration in both postures. However, only one active joint needs be rotated to change the mode from Straight to Dogleg, and so this mechanism has an electromagnetic brake to fix wheel rotation in this situation.

III. Statics

In this section, the static relations between the formation of the robot and actuator torques are described. Joint torques are obtained through a balance of force and moment acting on each part of the robot as well as the static characteristics of the differential gear units. This robot has a symmetrical structure, therefore the statics of one side of the mechanism is solved here. Forces and moments acting on the parts of the robot are shown in Fig. 7.

A. Torque Relation of Differential Gear Unit

When the differential gear unit is static, the torques of the two output axis are equal, and the torque of the carrier is

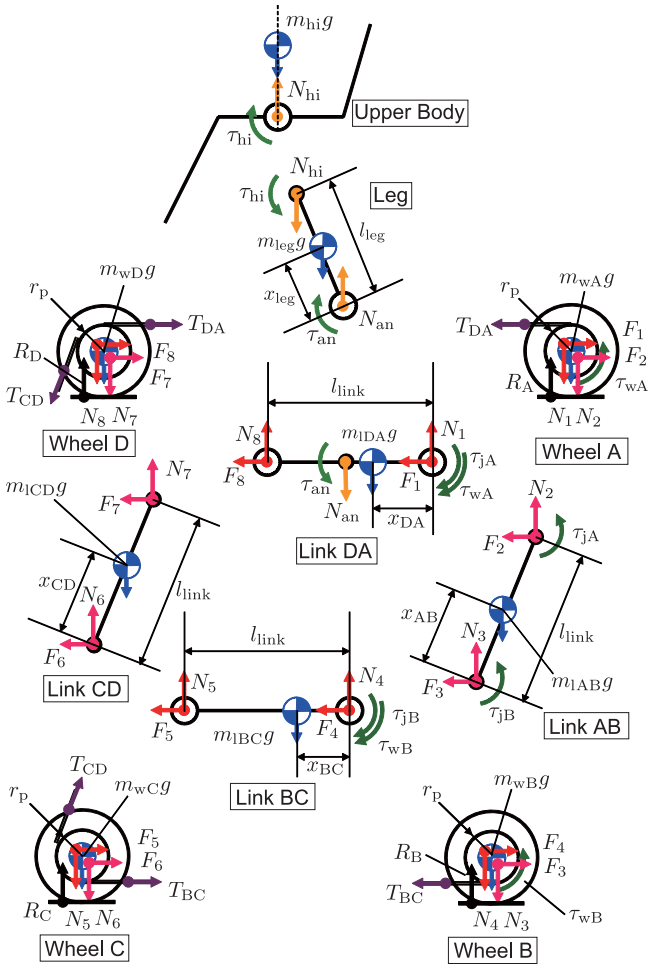

Fig. 7. Balance of force and moment on each part.

equal to the sum of the torques of the two output axis.

$$\tau_{ck} = 2\tau_{outk} \tag{1}$$

where τ_{ck} and τ_{outk} are the torques of the carrier and the output axis of differential gear unit k (k=A,B).

Relation between torques of motor and carrier is as follows:

$$\tau_{mA} = -\tau_{cA}/\gamma_{bg} \qquad \tau_{mB} = \tau_{cB}/\gamma_{bg} \tag{2}$$

where τ_{mA} and τ_{mB} are torques of motor A and B.

Relation among torques of output axis of the differential gear unit, wheels and joints of the four-bar linkage is as follows:

$$-\tau_{outA} = \frac{\tau_{jA}}{\gamma_{hj}} = \frac{\tau_{wA}}{\gamma_{hw}} \qquad \tau_{outB} = \frac{\tau_{jB}}{\gamma_{hj}\gamma_{sg}} = -\frac{\tau_{wB}}{\gamma_{hw}\gamma_{b}} \tag{3}$$

where τ_{wA}, τ_{wB}, τ_{jA} and τ_{jB} are torques of wheel A, wheel B, joint A and B.

From these, the following relation between the torques of the motor and the joints is obtained.

$$\tau_{mA} = \frac{2\tau_{jA}}{\gamma_{hj}\gamma_{bg}} \qquad \tau_{mB} = \frac{2\tau_{jB}}{\gamma_{hj}\gamma_{sg}\gamma_{bg}} \tag{4}$$

B. Static Balance of Each Part

Static balance of vertical forces on upper body and balance of moments about the hip joint is as follows:

$$N_{hi} = m_{hi}g \qquad \tau_{hi} = 0 \tag{5}$$

where N_{hi} is reaction forces on hip joint along Z axis, m_{hi} is the weight of the upper body including passenger's weight, g is acceleration of gravity, τ_{hi} is torque of hip joint.

Static balance of vertical forces on the leg and the balance of moments about the ankle joint is as follows:

$$\begin{aligned} N_{an} &= N_{hi} + m_{leg}g \\ \tau_{an} &= (N_{hi}l_{leg} + m_{leg}x_{leg}g)\sin\theta_{hi} + \tau_{hi} \end{aligned} \tag{6}$$

where N_{an} is reaction forces on ankle joint along Z axis, m_{leg} is weight of the leg part, l_{an} is length of the leg, x_{an} is the distance of the center of gravity of the leg from ankle joint.

Static balance of forces on the link DA and the balance of moments about joint A is as follows:

$$N_1 + N_8 - N_{an} - m_{lDA}g = 0 \qquad F_1 + F_8 = 0 \tag{7}$$

$$\begin{aligned} &-\tau_{jA} - \tau_{wA} - l_{link}(N_8\cos\theta_1 + F_8\sin\theta_1) \\ &\quad + 0.5N_{an}l_{link}\cos\theta_1 + \tau_{an} + m_{lDA}gx_{DA}\cos\theta_1 = 0 \end{aligned} \tag{8}$$

where N_1 and F_1 are reaction forces between link DA and joint A, N_8 and F_8 are reaction forces between link DA and joint D, m_{lDA} is the weight of link DA, l_{link} is link length, x_{DA} is the distance of the center of gravity of the link DA from joint A. Moreover, $\theta_1 = \theta_{hi} + \theta_{an}$.

Static balance of forces on wheel A and balance of moments about joint A is as follows:

$$\begin{aligned} -N_1 - N_2 - m_{wA}g + R_A - T_{DA}\sin\theta_1 &= 0 \\ -F_1 - F_2 + T_{DA}\cos\theta_1 &= 0 \\ \tau_{wA} + r_pT_{DA} &= 0 \end{aligned} \tag{9}$$

where N_2 and F_2 are reaction forces between link AB and joint A, m_{wA} is the weight of wheel A, R_A is ground reaction force on wheel A, T_{DA} is the tension of the chain connecting wheel D and A, r_s is the radius of the pulley.

Static balance of forces on link AB and balance of moments about joint B is as follows:

$$N_2 + N_3 - m_{lAB}g = 0 \qquad F_2 + F_3 = 0 \tag{10}$$

$$\tau_{jA} + \tau_{jB} - l_{link}(N_2\cos\theta_2 + F_2\sin\theta_2) + m_{lAB}gx_{AB}\cos\theta_2 = 0 \tag{11}$$

where N_3 and F_3 are reaction forces between link AB and joint B, m_{lAB} is the weight of link AB, x_{AB} is the distance of the center of gravity of the link AB from joint B. Moreover, $\theta_2 = \theta_1 + \phi_{jA}$.

Static balance of forces on wheel B and balance of moments about joint B is as follows:

$$\begin{aligned} -N_3 - N_4 - m_{wB}g + R_B - T_{BC}\sin\theta_3 &= 0 \\ -F_3 - F_4 + T_{BC}\cos\theta_3 &= 0 \\ \tau_{wB} - r_pT_{BC} &= 0 \end{aligned} \tag{12}$$

where N_4 and F_4 are reaction forces between link BC and joint B, m_{wB} is the weight of the wheel B, R_B is ground

reaction force on wheel B, T_{BC} is the tension of the chain connecting wheel B and C. Moreover, $\theta_3 = \theta_2 + \phi_{jB} - \pi$.

Static balance of forces on link BC and balance of moments about joint B is as follows:

$$N_4 + N_5 - m_{lBC} g = 0 \qquad F_4 + F_5 = 0 \tag{13}$$

$$-\tau_{jB} - \tau_{wB} - l_{link}(N_5 \cos\theta_3 + F_5 \sin\theta_3) + m_{lBC} g x_{BC} \cos\theta_3 = 0 \tag{14}$$

where N_5 and F_5 are reaction forces between link BC and joint C, m_{lBC} is the weight of the link BC, x_{BC} is the distance of the center of gravity of the link BC from joint B.

Static balance of forces on wheel C and balance of moments about joint C is as follows:

$$\begin{aligned} -N_5 - N_6 - m_{wC} g + R_C + T_{BC} \sin\theta_3 - T_{CD} \sin\theta_4 = 0 \\ -F_5 - F_6 - T_{BC} \cos\theta_3 + T_{CD} \cos\theta_4 = 0 \\ r_p T_{BC} - r_p T_{CD} = 0 \end{aligned} \tag{15}$$

where N_6 and F_6 are reaction forces between link CD and joint C, m_{wC} is the weight of the wheel C, R_C is ground reaction force on wheel C, T_{CD} is tension of the chain connecting wheel C and D. Moreover, $\theta_4 = \theta_3 + \phi_{jC}$.

Static balance of forces on link CD and balance of moments about joint C is as follows:

$$N_6 + N_7 - m_{lCD} g = 0 \qquad F_6 + F_7 = 0 \tag{16}$$

$$-l_{link}(N_7 \cos\theta_4 + F_7 \sin\theta_4) + m_{lCD} g x_{CD} \cos\theta_4 = 0 \tag{17}$$

where N_7 and F_7 are reaction forces between link CD and joint D, m_{lCD} is the wight of the link CD, x_{CD} is the distance of the center of gravity of the link CD from joint C.

Static balance of forces on wheel D and balance of moments about joint D is as follows:

$$\begin{aligned} -N_7 - N_8 - m_{wD} g + R_D + T_{CD} \sin\theta_4 + T_{DA} \sin\theta_1 = 0 \\ -F_7 - F_8 - T_{CD} \cos\theta_4 - T_{DA} \cos\theta_1 = 0 \\ r_p T_{CD} - r_p T_{DA} = 0 \end{aligned} \tag{18}$$

where m_{wD} is the weight of the wheel and shaft D, R_D is ground reaction force on wheel D.

A static solution can be obtained from solving these relation in each posture.

C. Static Solution

1) Hip and Ankle Joint: From (25) and (26), joint and motor torque of hip and ankle joint are obtained as follows:

$$\tau_{hi} = 0 \qquad \tau_{mhi} = 0 \tag{19}$$

$$\begin{aligned} \tau_{an} &= (m_{hi} l_{leg} + m_{leg} x_{leg}) g \sin\theta_{hi} \\ \tau_{man} &= \frac{1}{\gamma_{an}} (m_{hi} l_{leg} + m_{leg} x_{leg}) g \sin\theta_{hi} \end{aligned} \tag{20}$$

where τ_{mhi} and τ_{man} are motor torques of hip and ankle joint, γ_{an} is the gear ratio of the ankle joint.

2) Parallelogram Mode: When the four-bar linkage module is in Parallelogram mode, joint torques and motor torques are obtained with each combination of two grounding wheels.

When wheel A and B ground, from $R_C = R_D = 0$, following solution is obtained.

$$\tau_{jB} = \frac{\gamma_{sg}}{\gamma_{sg} + \gamma_b} \left\{ \left(m_{lDA} x_{DA} + m_{lBC} x_{BC} + (m_{wC} + m_{lCD} + m_{w\,D} + \frac{m_{hi} + m_{leg}}{2}) l_{link} \right) g \cos\theta_1 + \tau_{an} \right\} \tag{21}$$

$$\tau_{mA} = \tau_{mB} = \frac{2}{(\gamma_{sg} + \gamma_b)\gamma_{hj}\gamma_{bg}} \left\{ \left(m_{lDA} x_{DA} + m_{lBC} x_{BC} + (m_{wC} + m_{lCD} + m_{w\,D} + \frac{m_{hi} + m_{leg}}{2}) l_{link} \right) g \cos\theta_1 + \tau_{an} \right\} \tag{22}$$

In the same way, when wheel B and C ground, from $R_D = R_A = 0$, following solution is obtained.

$$\tau_{jB} = -\frac{\gamma_{sg}}{\gamma_{sg} + \gamma_b} \left\{ m_{lCD} x_{CD} + m_{lAB} x_{AB} + (m_{wD} + m_{lAD} + m_{w\,A} + m_{hi} + m_{leg}) l_{link} \right\} g \cos\theta_2 \tag{23}$$

$$\tau_{mA} = \tau_{mB} = -\frac{2}{(\gamma_{sg} + \gamma_b)\gamma_{hj}\gamma_{bg}} \left\{ m_{lCD} x_{CD} + m_{lAB} x_{AB} + (m_{wD} + m_{lAD} + m_{w\,A} + m_{hi} + m_{leg}) l_{link} \right\} g \cos\theta_2 \tag{24}$$

When wheel C and D ground, from $R_A = R_B = 0$, following solution is obtained.

$$\tau_{jB} = -\frac{\gamma_{sg}}{\gamma_{sg} + \gamma_b} \left\{ \left(m_{lDA} (l_{link} - x_{DA}) + m_{lBC} (l_{link} - x_{BC}) + (m_{wA} + m_{lAB} + m_{w\,B} + \frac{m_{hi} + m_{leg}}{2}) l_{link} \right) g \cos\theta_1 - \tau_{an} \right\} \tag{25}$$

$$\tau_{mA} = \tau_{mB} = -\frac{2}{(\gamma_{sg} + \gamma_b)\gamma_{hj}\gamma_{bg}} \left\{ \left(m_{lDA} (l_{link} - x_{DA}) + m_{lBC} (l_{link} - x_{BC}) + (m_{wA} + m_{lAB} + m_{w\,B} + \frac{m_{hi} + m_{leg}}{2}) l_{link} \right) g \cos\theta_1 - \tau_{an} \right\} \tag{26}$$

When wheel D and A ground, from $R_B = R_C = 0$, following solution is obtained.

$$\tau_{jB} = \frac{\gamma_{sg}}{\gamma_{sg} + \gamma_b} \left\{ m_{lCD} (l_{link} - x_{CD}) + m_{lAB} (l_{link} - x_{AB}) + (m_{wB} + m_{lBC} + m_{w\,C}) l_{link} \right\} g \cos\theta_2 \tag{27}$$

$$\tau_{mA} = \tau_{mB} = \frac{2}{(\gamma_{sg} + \gamma_b)\gamma_{hj}\gamma_{bg}} \left\{ m_{lCD} (l_{link} - x_{CD}) + m_{lAB} (l_{link} - x_{AB}) + (m_{wB} + m_{lBC} + m_{w\,C}) l_{link} \right\} g \cos\theta_2 \tag{28}$$

3) Dogleg Mode: When the four-bar linkage module is in Dogleg mode, joint and motor torques are obtained with each not-grounding wheel.

When wheel A does not ground, from $R_A = 0$, the following solution is obtained.

$$\tau_{jB} = \frac{\gamma_{sg}\gamma_{hj}}{\gamma_{sg}\gamma_{hj} - \gamma_b\gamma_{hw}} \left\{ \left(m_{lDA}(l_{link} - x_{DA}) + m_{lAB}x_{AB} + (m_{wA} + \frac{m_{hi} + m_{leg}}{2}) l_{link} \right) g\cos\theta_1 - \tau_{an} \right\} \quad (29)$$

$$\tau_{mA} = \tau_{mB} = \frac{2}{(\gamma_{sg}\gamma_{hj} - \gamma_b\gamma_{hw})\gamma_{bg}} \left\{ \left(m_{lDA}(l_{link} - x_{DA}) + m_{lAB}x_{AB} + (m_{wA} + \frac{m_{hi} + m_{leg}}{2}) l_{link} \right) g\cos\theta_1 - \tau_{an} \right\} \quad (30)$$

In the same way, when wheel B does not ground, from $R_B = 0$, following solution is obtained.

$$\tau_{jB} = \frac{\gamma_{sg}}{\gamma_b} \frac{\gamma_{hj}}{\gamma_{hj} + \gamma_{hw}} \left(m_{lAB}(l_{link} - x_{AB}) + m_{lBC}(l_{link} - x_{BC}) + m_{wB}l_{link} \right) g\cos\theta_2 \quad (31)$$

$$\tau_{mA} = \tau_{mB} = \frac{2}{(\gamma_{hj} + \gamma_{hw})\gamma_b\gamma_{bg}} \left(m_{lAB}(l_{link} - x_{AB}) + m_{lBC}(l_{link} - x_{BC}) + m_{wB}l_{link} \right) g\cos\theta_2 \quad (32)$$

When wheel C does not ground, from $R_C = 0$, following solution is obtained.

$$\tau_{jB} = \frac{\gamma_{sg}\gamma_{hj}}{\gamma_{sg}\gamma_{hj} - \gamma_b\gamma_{hw}} \left(m_{lBC}x_{BC} + m_{lCD}(l_{link} - x_{CD}) + m_{wC}l_{link} \right) g\cos\theta_3 \quad (33)$$

$$\tau_{mA} = \tau_{mB} = \frac{2}{(\gamma_{sg}\gamma_{hj} - \gamma_b\gamma_{hw})\gamma_{bg}} \left(m_{lBC}x_{BC} + m_{lCD}(l_{link} - x_{CD}) + m_{wC}l_{link} \right) g\cos\theta_3 \quad (34)$$

When wheel D does not ground, from $R_D = 0$, following solution is obtained.

$$\tau_{jB} = \frac{\gamma_{sg}}{\gamma_b} \frac{\gamma_{hj}}{\gamma_{hj} + \gamma_{hw}} \left\{ \left(m_{lDA}x_{DA} + m_{lCD}x_{CD} + (m_{wD} + \frac{m_{hi} + m_{leg}}{2}) l_{link} \right) g\cos\theta_1 + \tau_{an} \right\} \quad (35)$$

$$\tau_{mA} = \tau_{mB} = \frac{2}{(\gamma_{hj} + \gamma_{hw})\gamma_b\gamma_{bg}} \left\{ \left(m_{lDA}x_{DA} + m_{lCD}x_{CD} + (m_{wD} + \frac{m_{hi} + m_{leg}}{2}) l_{link} \right) g\cos\theta_1 + \tau_{an} \right\} \quad (36)$$

IV. Experiments

A. Specifications of Developed Prototype.

The specifications and dimensions of the developed prototype "TBW-1" are shown in Table I and Fig. 8.

This prototype has 1 DC servo motor in each hip and ankle joint, with 2 motors in the right and left four-bar linkage modules. The total system has 6 motors. It has 1 negative operation electromagnetic brake in the right and left four-bar linkage modules to fix the joint angle when the robot runs over even terrain. Negative-operation electromagnetic brakes are also fitted to the motors for the hip and ankle joints. The total height can be varied from 744 mm to 1460 mm by controlling the hip and ankle joints and the formation of the four-bar linkages. This enables the seat of the robot to be set at the same height as a standard wheelchair, and also bring the user's eye level up to the height of a standing person's. In both of the two formations shown in Fig. 8, 4 wheels are grounded, and the robot can run straight and turn around.

TABLE I
Specifications.

Model No.	TBW-1
Dimension / Weight	
Height	744 - 1460 mm
Width	1129 mm
Weight	154 kg (w/o electric component)
Mechanism	
Link Mechanism	Four-Bar Linkage
Degree of Freedom	6
Actuator	
Motor	DC servo motor
Rated Power	150 W
Brake	Electromagnetic Brake
Computer / Electric System	
CPU	PentiumM 1.8 GHz
DC Servo Driver Type	TD12770-48W10

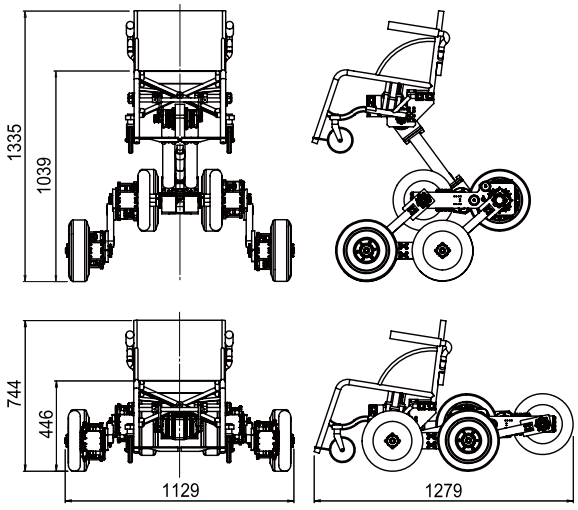

Fig. 8. Dimensions.

B. Experiments

To evaluate basic performance in ascending and descending stairs, an experiment in descending stairs was conducted at the entrance of a building at the authors' university. The riser height is 110 mm and the depth of the tread is 300 mm.

Currently, because this prototype had no sensors to measure the dimensions of the stairs, the joint angle transitions were set manually using inverse kinematics [11].

Sequential photographs of this experiment are shown in Fig. 9. At the beginning, the four-bar linkage modules are in Straight mode (0 s). The modules have transformed into Dogleg mode (0-16 s), the upper body has moved forward,

Fig. 9. Photos of the experiment descending stairs. (Riser height: 110 mm, tread depth: 300 mm)

and the four-bar linkage has transformed into Straight mode again by lifting the rear two wheels up (16-32 s). After that, the robot descends 4 steps by repeating the transformation between Parallelogram mode and Straight mode 4 times (32-80 s, 80-112 s, 112-176 s, 176-208 s). Finally, it has lifted the rear two wheels up (208-224 s). Although the descending speed was not fast, it can be said that the robot descended the stairs stably.

From this experimental result, it has been confirmed that the developed four-bar linkage module can transform smoothly between Straight mode and the other 2 modes, and the prototype could descend stairs stably by using this transformation.

Although it has not been confirmed experimentally, the robot can descend a longer flight of stairs by repeating transformation, and also ascend stairs by reversing these motions.

V. Conclusions and Future Work

In this paper, the necessity of the development of a barrier-free method that do not damage authenticity in an historical heritage environment, and mobility aid technology for elderly and handicapped people that has minimal invasiveness for use in an historical environment are described. With this goal in mind, a novel multiwheel stair-climbing wheelchair with variable configuration four-bar linkage is proposed, and its mechanical design, principle of operation, kinematics and statics are illustrated. Through experiments, basic performance in descending stairs has been confirmed.

In a future paper, several further experimental results to confirm the basic performance in ascending and descending stairs, including evaluation of ground pressure, force on the stair edge and running performance when driving all-wheels, will be reported upon. Based on this study, a sensing method for the dimensions of the stairs, a motion planning method, and a stabilization control method need to be studied. Finally, an evaluation of the robot's invasiveness through experiments in an actual heritage environment to clarify the problems that need to be solved in order to realize practical application are also future projects.

References

[1] D. Chhabra, et al., Staged Authenticity and Heritage Tourism. *Annals of Tourism Res.*, Vol. 30, No. 3, pp. 702–719, 2003.
[2] D. Davies et al., Continuous high-speed climbing control and leg mechanism for an eight-legged stair-climbing vehicle, *Proc. of the AIM2009*, pp. 1606–1612, 2009.
[3] A. Gonzalez et al.,On the Kinematic Functionality of a Four-Bar based Mechanism for Guiding Wheels in Climbing Steps and Obstacles, *Mechanism and Machine Theory*, Vol. 44, pp. 1507–1523, 2009.
[4] S. Hirose et al., Coupled drive of the multi-DOF robot, *Proc. of the ICRA 1989*, pp. 1610–1616, 1989.
[5] S. Hirose et al., Design of terrain adaptive versatile crawler vehicle HELIOS-VI, *Proc. of the IROS 2001*, pp. 1540–1545, 2001.
[6] Kanto Auto Works Ltd., All Wheel Drive Powered Wheelchair, 2004. URL `http://www.kanto-aw.co.jp/en/products/wheelchair/`.
[7] J. Y. Kim et al., Experimental realization of dynamic walking for a human-riding biped robot, HUBO FX-1. *Advanced Robotics*, 21(3-4): 461–484, 2007.
[8] Independence Technology L.L.C., Independence iBOT 3000 mobility system, 2003. URL `http://www.independencenow.com/ibot/`.
[9] M. Miyagi et al., Development of stair climbing wheelchair with legs and wheel system (1st report). *J. of the JSPE*, 64(3):403–407, 1998. (in Japanese).
[10] Y. Sugahara et al., Walking Up and Down Stairs Carrying a Human by a Biped Locomotor with Parallel Mechanism, *Proc. of the IEEE/RSJ IROS 2005*, pp. 3425-3430, 2005.
[11] Y. Sugahara et al., A Novel Stair-Climbing Wheelchair with Variable Configuration Four-Bar Linkage: Mechanism Design and Kinematics, *ROMANSY 18*, pp. 167-174, 2010.
[12] J. P. Taylor., Authenticity and sincerity in tourism. *Annals of Tourism Res.*, Vol. 28, No. 1, pp. 7–26, 2001.
[13] Top Chair SAS., The stair climbing wheelchair, 2003. URL `http://pagesperso-orange.fr/topchair/index_en.htm`.
[14] Toyota Motor Corporation., Toyota.co.jp -toyota partner robot-, 2004. URL `http://www.toyota.co.jp/en/special/robot/`.
[15] Y. Uchida et al., Fundamental performance of 6 wheeled off-road vehicle "HELIOS-V". *Proc. of the ICRA 1999*, pp. 2336–2341, 1999.
[16] Y. Utaka., Tourism and barrier free aspects of heritage sites: Case study on the world heritage sites in japan. In *Annual Conf. of Asia Pacific Tourism Association*, 2005.
[17] M. Vukobratović et al., On the stability of anthropomorphic system. *Mathematical Biosciences*, Vol. 15, pp. 1–37, 1972.
[18] N. Yanagihara et al., Mechanical analysis of a stair-climbimg wheelchair using rotary cross arm with wheels. *Proc. of the 17th Annual Conf. of the RSJ*, 1999. (in Japanese).
[19] N. Yoshida., A study on improvement of barrier-free devices at the heritage. In *Sum. of Tech. Papers of Annual Meeting Architectural Institute of Japan*, pp. 699–700, 2002. (in Japanese).
[20] J. Yuan et al., Actualization of safe and stable stair climbing and three dimensional locomotion for wheelchair. *Proc. of the IROS 2005*, pp. 2391–2396, 2005.